RECENT BREMSSTRAHLUNG MEASUREMENTS FROM THE SUPERCONDUCTING ELECTRON CYCLOTRON RESONANCE ION SOURCE VENUS

J. Y. Benitez#, C. M. Lyneis, L. W. Phair, D. S. Todd, D. Z. Xie
LBNL, Berkeley, CA 94720, USA

Abstract

Axial bremsstrahlung from the superconducting Electron Cyclotron Resonance ion source VENUS have been systematically measured as a function of RF heating frequency, and the axial and radial field strengths. The work focuses on bremsstrahlung with energies greater than 10 keV to extract the spectral temperature T_s. The three axial coils and the radial coils in the superconducting VENUS can all be set independently and have a large dynamic range, which makes it possible to decouple B_{min} and ∇B_{ECR} and study their effects on the bremsstrahlung independently. With typical pressure and RF power levels, the measurements show that T_s depends approximately linearly on B_{min} and is not correlated with the ∇B_{ECR}, the magnetic field mirror ratios, or the RF frequency. These results are important for the next generation of ECR ion sources, which are designed to operate at frequencies above 40 GHz and significantly higher magnetic fields where bremsstrahlung is expected to cause a significant cryogenic heat load and increase the radiation shielding requirements.

INTRODUCTION

Electron Cyclotron Resonance Heating (ECRH) is an efficient method to couple microwave energy into the plasma electrons. Use of ECRH to generate plasma began with the early mirror machines developed by the plasma fusion community and later as a spin-off in the high charge state ECR ion sources, ECRIS, initially developed by R. Geller in the 1970's [1]. VENUS is the first 3rd generation ECR ion source using both 18 and 28 GHz microwave power to produce a plasma with electrons of sufficient energy to produce high charge states such as Ar^{18+} [2], Xe^{43+}, and U^{50+} [3]. The ionization potential for these highly-charged ions is in the range of 2 to 5 keV and the maximum cross section for electron impact ionization occurs at three to five times those energies or approximately 6 to 25 keV. VENUS produces plasma with electrons of maximum energy up to several hundred keV as is evidenced in the hot tail of the emitted bremsstrahlung. The existence of the electron hot tail has been observed in both simple mirror machines for fusion research in the 60's [4] and in the minimum B magnetic field structures used in modern high charge state ECR ion sources [5].

The performance of high charge state ECR ion sources scales roughly with the square of RF heating frequency, as predicted by R. Geller [6]. The third generation ECRIS operating at either 24 or 28 GHz [2, 7-9] are presently the best performers. These sources operate at higher magnetic fields than earlier generation sources operating at frequencies of 18 GHz or lower. The third generation ECRIS also produce significantly more intense and more energetic bremsstrahlung. The high energy bremsstrahlung adds a thermal load to the cryogenic system for superconducting ECRIS because the high energy x-rays (~ E > 300 keV) easily pass through the plasma chamber and outer wall of the cryostat and then are absorbed in the cold mass [5]. The fourth generation sources currently being developed will operate at higher magnetic fields with heating frequencies above 40 GHz [10]. It is anticipated that the next generation source will produce even more intense and energetic hot electrons and therefore methods to understand, control, or reduce the bremsstrahlung production are needed. This research explores which ECRIS parameters including magnetic field geometry and microwave frequency affect the production of bremsstrahlung and the spectral temperature T_s obtained from it.

EXPERIMENTAL SETUP

VENUS uses three superconducting solenoids and one superconducting sextupole to generate the minimum-B magnetic field configuration to confine the plasma, as shown in Figure 1. Each coil is independently powered and the axial fields can produce up to 4 T at injection, 3T at extraction and a center coil that can produce a B_{min} value from 0 to 2 T. The sextupole coils can produce up to 2.2 T on the plasma wall at a radius of 72 mm and the radial field generated by the sextupole is typically set to values close to the peak axial field at extraction. This produces a closed resonance field at 2T or twice B_{ECR} at 28 GHz [11].

The central field can be lowered sufficiently so there are simultaneous resonance fields for 14, 18 and 28 GHz. The VENUS microwave system consists of a 2 kW 18 GHz klystron and a 10 kW 28 GHz gyrotron. A 2 kW 14 GHz klystron was also used briefly to test the frequency dependence of the spectral temperature.

The axially emitted bremsstrahlung spectra from VENUS were recorded using an Amptek XR-100-CdTe X-Ray and Gamma Ray diode detector [12]. It consist of a 1 mm thick, 25 mm^2 detector that sits behind a 4 mil Be window. Its resolution at 122 keV is < 1.5 keV FWHM, which is not as good as Si diode detectors. However, the CdTe detectors are much more sensitive at energies above 20 keV as they have a higher stopping power with shorter attenuation lengths [13]. In addition, the XR-100-CdTe detector has the advantage that it can be operated in vacuum, without attenuation caused by windows.

#jybenitez@lbl.gov

ISBN 978-3-95450-186-1

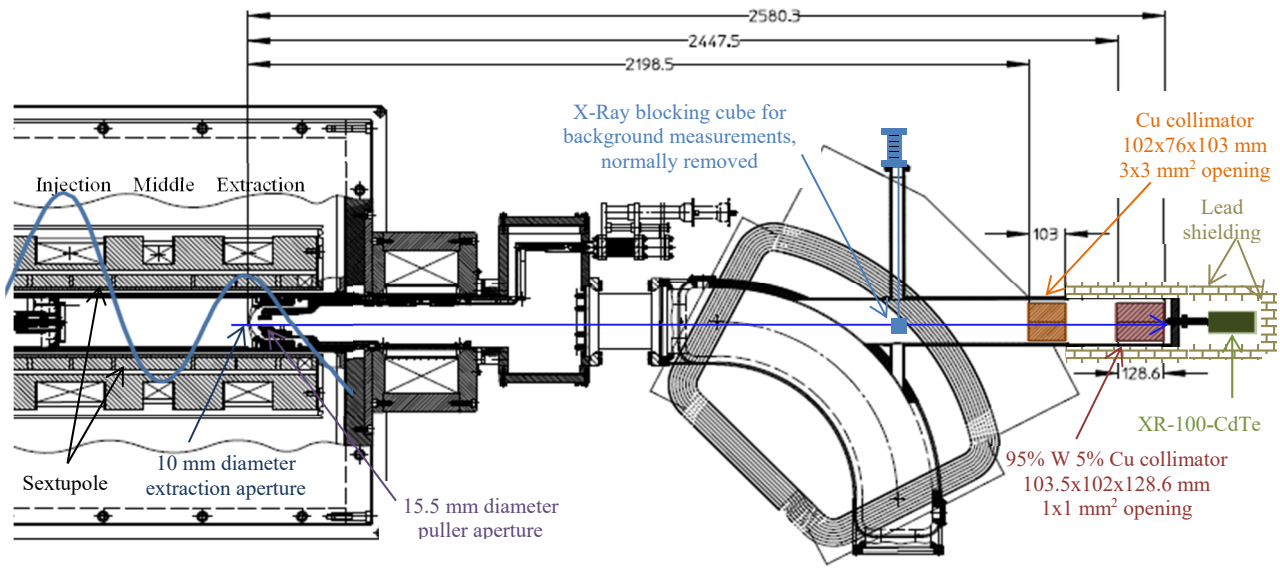

Figure 1: Schematic of the experimental setup of the XR-100-CdTe detector at the VENUS ion source. All units in mm.

From 4 keV to 80 keV the intrinsic efficiency, a ratio of the number of pulses recorded by the detector to the number of gamma rays hitting the detector, with the window taken into account, is above 80%. However, this paper includes x-rays measured between 10 keV to 300 keV. Between 80 keV and 300 keV the efficiency drops gradually to 10%. All spectra shown have been corrected for detector intrinsic efficiency which includes the correction for the 4 mil beryllium window on the detector. The detector's intrinsic efficiency was verified using various radioactive sources with known activities and compared well to that quoted by the manufacturer and this was used to make the corrections. The detector sits on the optical axis, in line with the extraction electrode center, and inside the vacuum chamber, as shown in Figure 1. Therefore, no corrections due to attenuation in air or through a window are necessary. The spectra are not corrected for the detector's photopeak efficiency, the probability of producing a full-energy peak. The detector's energy was calibrated used standard radioactive sources with known gamma lines.

Between the detector and the extraction aperture is a set of two collimators. The first sits directly up against the detector face and is a heavy metal (95% W and 5% Cu) block. It is 128.6 mm long and has a 1 mm square groove. The second collimator is 146 mm upstream of the first collimator and is solid Cu. It is 102 mm long with a 3 mm square groove. This corresponds to a square with 20 mm sides at the extraction electrode that is visible to the detector. The VENUS ion source has an aluminium extraction electrode. It is important to note that midway through the measurements, which spanned several months, the 10 mm diameter extraction aperture was replaced with a slightly thicker aluminium electrode at the aperture opening to improve heat transfer and prevent melting it. Analysis of spectra recorded before and after show that this only affected their shapes at the low energy end that is not considered in this paper. Although the new electrode decreases the total counts by up to 50%, the slope of the spectra in the energy range between 80 and 300 keV did not change.

The spectral temperature, T_s, is obtained from the recorded bremsstrahlung by fitting a straight line to the semi-logarithmic representation of the spectra over a selected energy. For this paper the energy range was approximately 80-120 keV. The T_s, taken as the reciprocal of the line's slope, is an indirect measure of the energy distribution of the plasma electrons and is used to characterize the temperature distribution and relative hot electron density in high charge state ECR plasma. This spectral temperature is not a direct measure of the electron energy distribution of the hot electrons in the plasma.

An x-ray blocking cube, shown in Figure 1 was installed to measure the background reaching the detector from outside the collimator apertures. When the 22 mm side cube, made from a tantalum-niobium alloy, is inserted, it blocks the x-rays from entering the collimators and reaching the detector. The remaining x-rays detected are indirectly scattered bremsstrahlung and can be subtracted as a background. The background spectrum below 100 keV is negligible but it does contribute a large percentage of the counts at higher energies and this affects the spectral temperature extracted from the data. When the background is subtracted from the original spectra, the spectral temperature is reduced by 2% to 20%.

EXPERIMENTAL RESULTS

Experiment Design

Aside from the magnetic field configuration and heating frequency the measurements were made with similar parameters through all data sets. All data was recorded at

ISBN 978-3-95450-186-1

a power level of 1000W, measured at the transmitter, for 14, 18, or 28 GHz heating frequency, and at similar oxygen gas pressure and bias disk voltage. The power was limited to 1000W to avoid unstable plasmas that can generate large fluctuations in the bremsstrahlung output. However, it was verified that T_s remained relatively constant up to a power level of 9000W as shown in Figure 2.

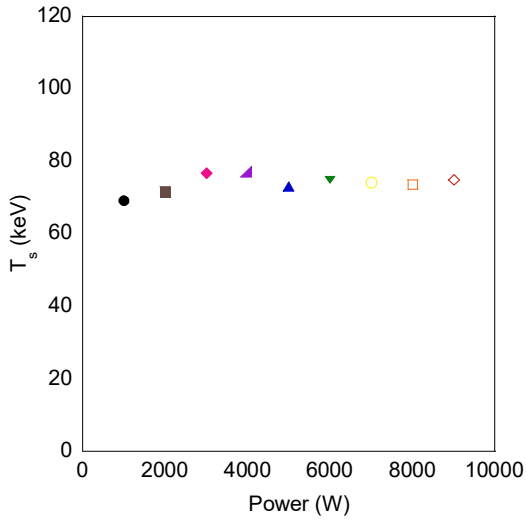

Figure 2: T_s obtained show essentially no change with increasing power from 1000 to 9000W at a fixed magnetic field configuration.

We focused on how the magnetic configuration and microwave heating frequencies affect the axial bremsstrahlung and resulting spectral temperature. The investigation was divided into three main sections. First, B_{min} was varied while the gradient at the resonance zone B_{ECR} was held approximately constant. Second, the gradient at the resonance zone B_{ECR} was varied while B_{min} was held constant. Third, we also compared spectra recorded at a fixed magnetic field configuration for three different heating frequencies.

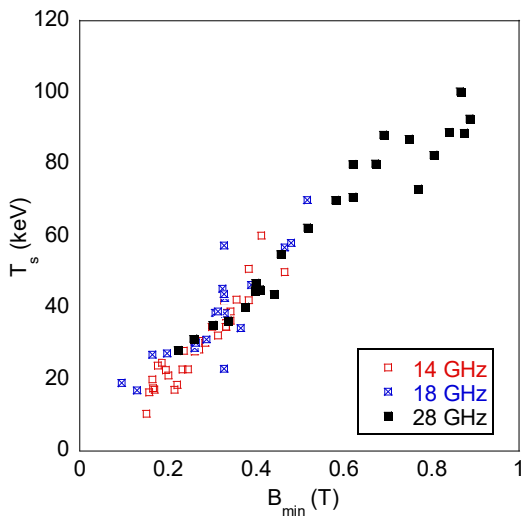

Figure 3: All data collected for VENUS is summarized in this table where T_s is plotted versus B_{min}.

The gradient at the resonance zone B_{ECR}, henceforth written as ∇B_{ECR}, is calculated on axis. Figure 3 shows graphically a summary of the measurements in which the T_s for all collected data is plotted versus the minimum center field B_{min} for three different independently used heating frequencies of 14, 18 and 28 GHz, at various field configurations and gradients. This summary plot clearly shows that the hot electron T_s depends linearly on B_{min} and does not depend on the RF heating frequency.

Constant Gradient at B_{ECR} while Varying B_{min}

In the first part of the investigation we held ∇B_{ECR} approximately constant and varied B_{min} for the three heating frequencies. For the case of 18 GHz heating, ∇B_{ECR} was varied by 9.1% while B_{min} was varied by 59.4%. The parameters used for 18 GHz heating are listed in Table 1. Also listed are the field parameters for the case of 28 GHz heating, in which ∇B_{ECR} was varied by 12.9% while B_{min} was varied by 81.8%. It is seen when ∇B_{ECR} is held approximately constant and B_{min} is varied this changes T_s significantly. The experiment was also done with 14 GHz heating frequency and similar results were seen. Figure 4 show the magnetic field configuration and T_s versus B_{min} for the 28 GHz settings.

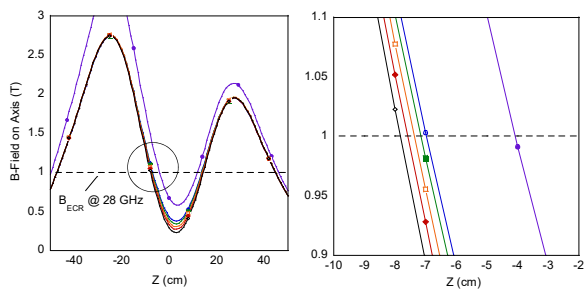

a.)

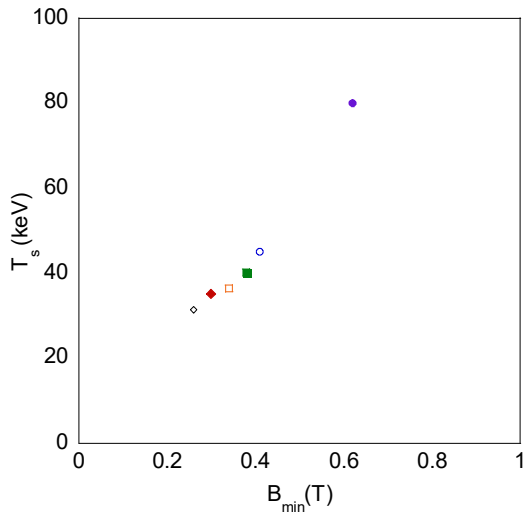

b.)

Figure 4: Using 28 GHz heating frequency a.) axial magnetic fields on axis for quasi-constant gradient at the resonance zone and b.) spectral temperatures.

ISBN 978-3-95450-186-1

Table 1: Magnetic Field Settings with Approximately Constant Gradient at the Resonance Zone and Variable B_{min} for 18 and 28 GHz Heating

f (GHz)	B_{min} on axis (T)	Inj. ∇B_{ECR} (T/m)	Ext. ∇B_{ECR} (T/m)	Ts (keV)
18	0.26	-7.5	6.77	30.2
	0.31	-8.16	6.44	38.9
	0.33	-7.64	7.03	38.5
	0.36	-7.54	6.44	46.6
	0.38	-7.45	6.32	55.0
	0.48	-7.71	6.54	58.0
28	0.26	-12.66	10.98	31.3
	0.30	-12.44	10.75	35.2
	0.34	-12.29	10.62	36.4
	0.38	-12.05	10.09	40.2
	0.41	-11.15	9.88	45.1
	0.62	-11.13	8.74	80.0

Constant B_{min} while Varying Gradient at B_{ECR}

In the second part of the investigation we held B_{min} constant and varied ∇B_{ECR} for 14 and 18 GHz. Figure 5a illustrates how ∇B_{ECR} was varied while maintaining a constant B_{min} for the 14 GHz tests. For 14 GHz heating, in order to vary ∇B_{ECR} the injection and extraction fields were varied from 1.64 T to 2.14 T and 1.07 T to 1.45 T, respectively. The minimum field and radial field were held constant and were 0.26 T and 1.0 T, respectively.

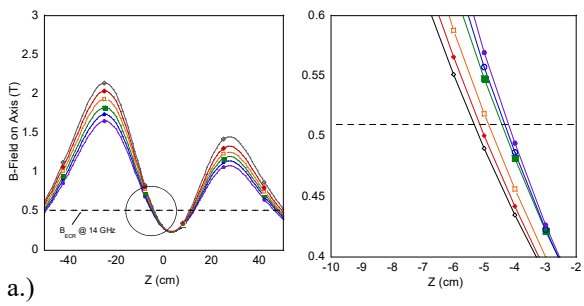

a.)

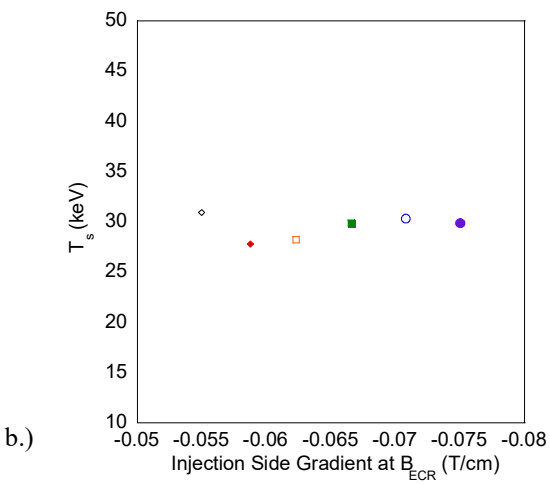

b.)

Figure 5: Using 14 GHz heating frequency a.) axial magnetic fields on axis when varying the gradient at the resonance zone and b.) spectral temperatures.

Column 5 of Table 2 shows that there is little variation in the spectral temperature while the gradient at injection is varied by 24% and at extraction by 20.6%. Figure 5b shows the resulting T_s versus B_{min} for the 14 GHz settings. For 18 GHz the injection and extraction fields were varied respectively from 1.67 T to 2.90 T and 1.14 T to 1.93 T, while minimum axial field and radial field were held constant at 0.33 T and 1.29 T, respectively. The spectral temperatures obtained using 18 GHz heating do not vary by more than 17% while the gradient at the injection was varied by 36%. The experiment was also done with 28 GHz heating frequency and similar results were seen.

Table 2: Magnetic Field Settings for Constant B_{min} While Varying Field Gradients at the Resonance Zone for 14 and 18 GHz Heating

f (GHz)	B_{min} on axis (T)	Inj.∇B_{ECR} (T/m)	Ext.∇B_{ECR} (T/m)	Ts (keV)
14	0.26	-6.3	5.09	30.9
	0.26	-5.94	5.40	27.8
	0.26	-6.30	5.40	28.2
	0.26	-6.69	5.66	29.9
	0.26	-7.15	6.14	30.3
	0.26	-7.58	6.26	29.9
18	0.33	-7.24	6.16	42.8
	0.33	-7.64	7.03	43.8
	0.33	-8.91	7.65	38.4
	0.33	-9.25	8.41	45.3

Comparison of Different Frequencies with Fixed Magnetic Field Values

Spectra were recorded at the same magnetic field configuration with each heating frequency 14, 18, and 28 GHz. Figure 6b shows spectra for a fixed magnetic field configuration. The shape of the spectra do not depend on the heating frequency used, although the count rate differs. For all spectra the RF power was set to 1 kW at the exit of the klystron or gyrotron. There was a mismatch in between the 14 GHz klystron and VENUS plasma chamber resulting in about 10% reflected power. However, our tests show that the spectral temperature was insensitive to small differences in RF power levels. While the magnetic field configuration was kept constant, for different heating frequencies this results in significantly different gradients at each resonance zone as shown in Table 3. For example in this test ∇B_{ECR} at injection changes from -4.67 T/m at 14 GHz to -12.75 T/m and the spectral temperature remain approximately constant. This supports the idea that the spectral temperature is not correlated with the value of the magnetic field gradient at resonance. Although only one set of measurements is presented, it was shown true for several configurations.

ISBN 978-3-95450-186-1

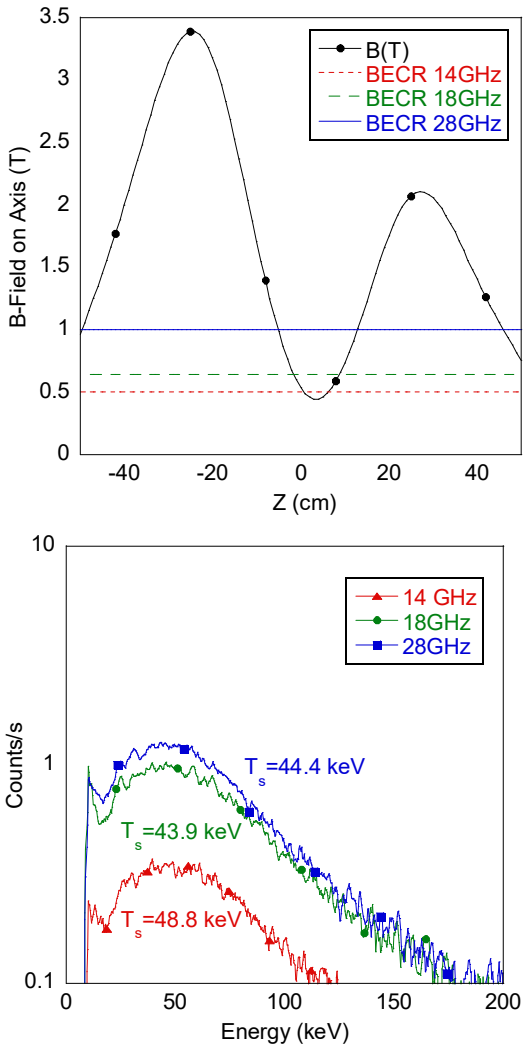

Figure 6: a.) Axial magnetic field on axis used for spectra recorded at 14, 18, and 28 GHz heating frequency. b.) Resulting spectra.

Variation of the Radial Magnetic Field

The radial field was also varied to see its effect on the spectral temperature. VENUS is typically operated with the radial field at the wall slightly less than the axial magnetic field at extraction and this was the magnetic field configuration used for most of the measurements reported.

Table 3: Results for Spectra Recorded with Each Heating Frequency at Identical Magnetic Field Configuration of Injection, Extraction, and Middle Axial Fields 3.39 T, 2.10 T and 0.48 T, respectively

Frequency (GHz)	**Injection** ∇B_{ECR} (T/m)	**Extraction** ∇B_{ECR} (T/m)	**Ts** (keV)
14	-4.67	4.22	48.8
18	-7.71	6.54	43.8
28	-12.75	10.00	44.4

Figure 7 shows the spectra and calculated values of the spectral temperature at 18 GHz with the injection, extraction, and middle fields set to 3.39 T, 2.1 T and 0.48 T, respectively while the radial field was varied while the radial field was varied from 1.29 T to 2.15 T. There was no significant shift in the spectral temperature or in the shape of the spectra and this indicates T_s remains unaffected as long as the radial field at the wall is lower than the maximum field at extraction. For these measurements, the value of the radial field quoted is that produced by the sextupole alone at the plasma wall. The magnitude of B at the wall is also influenced by the fields from the solenoids and varies across the plasma wall depending on both z and phi.

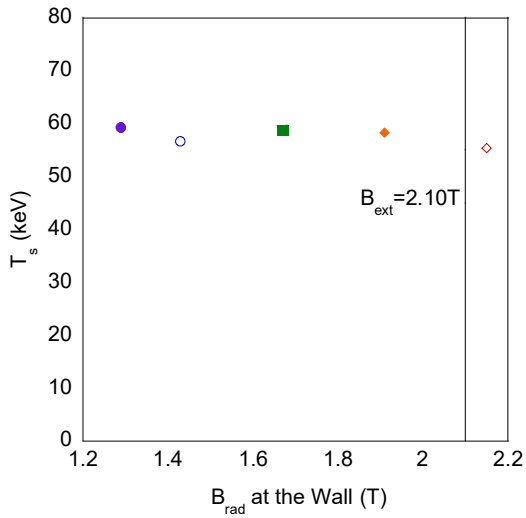

Figure 7: T_s for the 18 GHz operations with injection, extraction and middle field values of 3.39 T, 2.1 T and 0.48 T, respectively, while the radial field was varied from 1.29 T to 2.15 T.

In a second set of data the extraction field was lowered to 1.47 Tesla, the injection and middle field were held at 2.23 T and .33 T while the radial field was varied from 1.29 T to 2.15 T. With the extraction field set at 1.47 T, Figure 8 shows that both the intensity and shape of the spectra begin to increase and change when the radial field is increased to values well above the extraction field, which reduces the loss of electrons radially and enhances the loss in the extraction region.

In Figure 9 we investigated the dependence of T_s on B_{min} when the extraction field was set to values well below the field on the radial wall of the chamber. The data obtained when varying the radial field demonstrates that T_s still depends strongly B_{min} remains even when the weak point in confinement is shifted toward the extraction end. However the slope of T_s is different. These results can be related to the simulations discussed by Thuillier et al who present a simple model where the hot electrons are fully magnetized and follow the magnetic field lines [14]. The reference shows that a geometrical model studying where the field lines pass through the ECR zone and land on the chamber walls can be used to show how electrons escape

ISBN 978-3-95450-186-1

confinement at the regions where the magnetic field is weakest. Experimentally we have shown that by raising the radial field above the extraction field, the weak point in the magnetic confinement is shifted towards the extraction plate, thereby causing electrons to preferentially escape axially and collide at the extraction plate. This creates higher count rates with our axial detector and in one case at high microwave power excessive heat was dumped on the extraction plate damaging it.

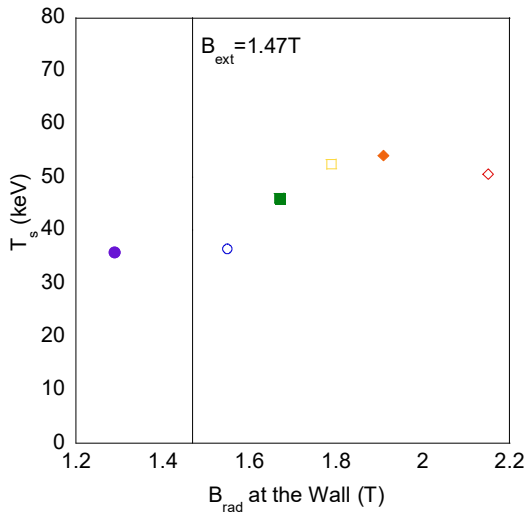

Figure 8: T_s for the 18 GHz operations with injection, extraction and middle field values of 2.23 T, 1.47 T and 0.33 T, respectively, while the radial field was varied from 1.29 T to 2.15 T.

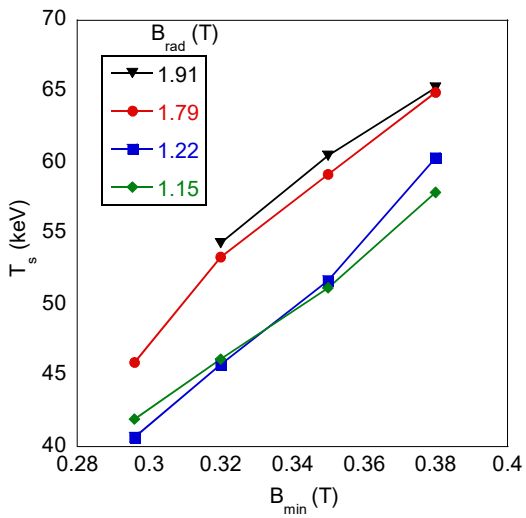

Figure 9: B_{min} is varied at each value of B_{rad}. When B_{rad} is raised above B_{ext} of 1.49 T the slope of the spectra changes with an increase in T_s but remains the proportional dependence on B_{min}.

DISCUSSION

There are two key results from the experimental measurements. First, the spectral temperature of the axial bremsstrahlung depends on the value of B_{min} and is not correlated with the value of ∇B_{ECR}. In a number of previous measurements, there appeared to be a correlation between ∇B_{ECR} and T_s, and this was thought to be evidence that at lower ∇B_{ECR} electron heating is more efficient. However, in these earlier studies both ∇B_{ECR} and B_{min} were changed at the same time [15-16].

The key difference in the measurements presented here is that the presence of a center coil in addition to the injection and extraction coils used in most other sources allows us to vary ∇B_{ECR} and B_{min} either together or with one held approximately fixed. It has often been observed that as an ECRIS is operated at higher frequencies the spectral temperature increases. Furthermore, it was typically thought that it was the ratio of B_{min}/B_{ECR} that was the important factor in determining T_s. These results show that T_s depends not on the ratio of B_{min} to B_{ECR}, but simply on the magnitude of B_{min}. This means that as new, higher frequency sources come into operation the generation of hot electrons can be controlled if B_{min} is not scaled up with frequency. In the case of the VENUS operation with B_{min} at about .4 T can produce excellent results without generating large amounts of high energy bremsstrahlung which can penetrate into the cold mass and generate an unwanted cryogenic heat load. Additionally, for fixed magnetic field geometry, T_s is independent of whether the RF frequency is 14, 18 or 28 GHz. This result strengthens the case that T_s is not correlated with ∇B_{ECR}, since with a fixed magnetic geometry, the value of ∇B_{ECR} is different for each frequency.

Further experimental measurements are planned to measure the axial bremsstrahlung at energies between 100 eV and 10 keV using a X-123 SDD detector from Amptek [17].

REFERENCES

[1] R. Geller, "Electron Cyclotron Resonance (E.C.R.) Multiply Charged Ion Sources," in *IEEE Transactions on Nuclear Science*, vol. 26, no. 2, pp. 2119-2127, April 1979.

[2] D. Xie *et al.*, "Recent production of intense high charge ion beams with VENUS," presented at ECRIS'16, Busan, Korea, August 2016, THAO01, these proceedings.

[3] J. Benitez *et al.*, "Production of high intensity ^{48}Ca for the 88-Inch Cyclotron and other updates," *Rev. Sci. Instrum.*, vol. 85, 02A961, 2014.

[4] T. Rognlien *et al.*, "Electron cyclotron resonance heating in tandem-mirror end cells," *Phys. Fluids B*, vol. 2, p. 338, 1990.

[5] D. Leitner *et al.*, "Measurement of the high energy component of the x-ray spectra in the VENUS electron cyclotron resonance ion source," *Rev. Sci. Instrum.*, vol. 79, 033302, 2008.

[6] R. Geller, *Electron Cyclotron Resonance Ion Sources and ECR Plasmas*. London, England, UK: Institute of Physics Publishing, 1996.

[7] L. Sun *et al.*, "Advancement of highly charged ion beam production by superconducting ECR ion source SECRAL (invited)," *Rev. Sci. Instrum.*, vol. 87, 02A707, 2016.

ISBN 978-3-95450-186-1

[8] G. Machicoane *et al.*, "First results at 24 GHz with the superconducting source for ions (SUSI)," in *Proc. of ECRIS'14*, Nizhny Novgorod, Russia, May 2014, paper MOOMMH03.
[9] Y. Higurashi *et al.*, "Recent development of RIKEN 28 GHz superconducting electron cyclotron resonance ion source," *Rev. Sci. Instrum.*, vol. 85, 02A953, 2014.
[10] C. Lyneis *et al.*, "Concept for a fourth generation electron cyclotron resonance ion source," *Rev. Sci. Instrum.*, vol. 83, 02A301, 2012.
[11] D. Hitz *et al.*, "Results and interpretation of high frequency experiments at 28 GHz in ECR ion sources, future prospects," *Rev. Sci. Instrum.*, vol. 73, 509, 2002.
[12] Amptek, http://amptek.com/products/xr-100t-cdte-x-ray-and-gamma-ray-detector/
[13] R. Redus *et al.*, "Combining CdTe and Si detectors for energy-dispersive x-ray fluorescence," *X-Ray Spectrom.*, vol. 41, p. 393, 2012.
[14] T. Thuillier *et al.*, "Investigation on the electron flux to the wall in the VENUS ion source," *Rev. Sci. Instrum.*, vol. 87, 02A736, 2016.
[15] H. Zhao *et al.*, "Effects of magnetic configuration on hot electrons in highly charged ECR plasma," *Plasma Sources Sci. Technol.*, vol. 18, 025021, 2009.
[16] C. Lyneis *et al.*, "Measurement of bremsstrahlung production and x-ray cryostat heating in VENUS," *Rev. Sci. Instrum.*, vol. 77, 03A342, 2006.
[17] Amptek, http://amptek.com/products/x-123sdd-complete-x-ray-spectrometer-with-silicon-drift-detector-sdd/

ISBN 978-3-95450-186-1